THE JOURNAL OF BIOLOGICAL CHEMISTRY VOL. 283, NO. 28, pp. 19540–19550, July 11, 2008

Rapid, Opioid-sensitive Mechanisms Involved in Transient Receptor Potential Vanilloid 1 Sensitization*[S]

Received for publication, September 20, 2007, and in revised form, May 8, 2008 Published, JBC Papers in Press, May 15, 2008, DOI 10.1074/jbc.M707865200

Irina Vetter[‡], Wei Cheng[§], Madusha Peiris[‡], Bruce D. Wyse[‡], Sarah J. Roberts-Thomson[‡], Jie Zheng[§], Gregory R. Monteith[‡], and Peter J. Cabot[‡1]

From the [‡]School of Pharmacy, The University of Queensland, St Lucia, Queensland 4072, Australia and the [§]Department of Physiology and Membrane Biology, School of Medicine, The University of California, Davis, California 95616

TRPV1 is a nociceptive, Ca^{2+}-selective ion channel involved in the development of several painful conditions. Sensitization of TRPV1 responses by cAMP-dependent PKA crucially contributes to the development of inflammatory hyperalgesia. However, the pathways involved in potentiation of TRPV1 responses by cAMP-dependent PKA remain largely unknown. Using HEK cells stably expressing TRPV1 and the μ opioid receptor, we demonstrated that treatment with the adenylate cyclase activator forskolin significantly increased the multimeric TRPV1 species. Pretreatment with the μ opioid receptor agonist morphine reversed this increased TRPV1 multimerization. FRET analysis revealed that treatment with forskolin did not cause multimerization of pre-existing TRPV1 monomers on the plasma membrane and that intracellular pools of TRPV1 exist mostly as monomers in this model. This suggests that increased TRPV1 multimerization occurred from an intracellular store of inactive TRPV1 monomers. Treatment with forskolin also caused an increase in TRPV1 expression on the plasma membrane not resulting from increased TRPV1 expression, and this rapid TRPV1 translocation was inhibited by treatment with morphine. Thus, potentiation of TRPV1 responses by cAMP-dependent PKA involves plasma membrane insertion of functional TRPV1 multimers formed from an intracellular store of inactive TRPV1 monomers. This potentiation occurs rapidly and can be dynamically modulated by activation of the μ opioid receptor under conditions where cAMP levels are raised, such as with inflammation. Increased translocation and multimerization of TRPV1 channels provide a cellular mechanism for fine-tuning of nociceptive responses that allow for rapid modulation of TRPV1 responses independent of transcriptional changes.

The ability to sensitize or desensitize painful stimuli is fundamental for survival. In inflammation, sensitization of peripheral nociception contributes to the development of hyperalgesia. Pro-inflammatory mediators including prostaglandins mediate an increase in cellular cAMP levels, which in turn leads to sensitization of nociception as a result of activation of cAMP-dependent protein kinase (PKA)[2] (1). Such sensitization may involve the transient receptor potential vanilloid 1 (TRPV1) (2).

TRPV1 is a calcium-permeable ion channel that is activated by the prototypical agonist capsaicin, the component that conveys the sensation of "heat" to chili peppers (3). Endogenous TRPV1 activators include lipophilic arachidonic acid metabolites such as *N*-arachidonoyl-dopamine and 12-hydroperoxyeicosatetraenoic acid (4, 5), but also heat and protons (3). TRPV1 and endovanilloid signaling are implicated in various inflammatory hyperalgesic conditions. The contribution of TRPV1 to inflammatory hyperalgesia has been established through observations that TRPV1 antagonists can dose-dependently reverse both thermal and mechanical inflammatory hyperalgesia (4, 5). In addition, thermal inflammatory hyperalgesia is significantly reduced in TRPV1 knock-out mice (6).

Several pro-inflammatory mediators and cytokines, including prostaglandin E2, sensitize TRPV1 responses under inflammatory conditions (7). Moreover, the TRPV1 is sensitized directly by cAMP-dependent PKA (8), making the TRPV1 a direct molecular target for the development of inflammatory hyperalgesia (2, 9). Although potentiation of TRPV1 responses by cAMP-dependent PKA appears crucial in the development of inflammatory hyperalgesia, the mechanisms underlying this potentiation are not fully understood.

Peripheral sensitization of nociceptive responses represents a cellular process to encourage rest and recovery after injury. The ability to modify responses rapidly, without having to rely on altering expression levels of nociceptive receptors, is essential for rapid adaption to external circumstances. This system is exemplified by the release of endogenous opioids from immune cells, which affects analgesia in inflamed tissues (10), and the increased effectiveness of exogenous opioids in inflammation (11). The capacity for rapid fine-tuning and modulation of sensitized nociception is further demonstrated by the ability of opioids to inhibit TRPV1-mediated capsaicin responses potentiated by cAMP-dependent PKA (12). To date, no mechanism has been proposed to

* This work was supported, in whole or in part, by National Institutes of Health Grant REY016754A. This work was also supported by an NHMRC Dora Lush Biomedical Research Scholarship (to I. V.) and the American Heart Association (0665201Y) (to J. Z.). The costs of publication of this article were defrayed in part by the payment of page charges. This article must therefore be hereby marked "*advertisement*" in accordance with 18 U.S.C. Section 1734 solely to indicate this fact.

[S] The on-line version of this article (available at http://www.jbc.org) contains supplemental Figs. S1–S5.

[1] To whom correspondence should be addressed: School of Pharmacy, The University of Queensland, St Lucia 4072, Australia. Tel.: 61-7-3365-1376; Fax: 61-7-3365-1688; E-mail: p.cabot@uq.edu.au.

[2] The abbreviations used are: PKA, cAMP-dependent kinase; TRPV1, transient receptor potential vanilloid 1; HEK, human embryonic kidney cells; FRET, fluorescence resonance energy transfer; MOP, μ opioid receptor; RTX, resiniferatoxin; PSS, physiological salt solution; FSK, forskolin; DRG, dorsal root ganglion; PBS, phosphate-buffered saline; BSA, bovine serum albumin; ANOVA, analysis of variance; MTS, 3-(4,5-dimethylthiazol-2-yl)-5-(3-carboxymethoxyphenyl)-2-(4-sulfophenyl)-2H-tetrazolium.

explain how TRPV1 sensitization by cAMP-dependent PKA can be achieved in a manner that provides for rapid potentiation while maintaining the capacity for dynamic modulation.

Here, we present evidence for a model that describes how, as a consequence of activation of adenylate cyclase, an intracellular pool of inactive TRPV1 monomers is transported to the plasma membrane where they function as TRPV1 multimers. This mechanism incorporates 2-fold regulation involving both altered multimerization and trafficking. It provides the basis for rapid modulation of nociceptive TRPV1 responses and fine-tuning of nociception. Modification of this pathway by the opioid receptor agonist morphine can rapidly alter TRPV1 potentiation and thus allows dynamic regulation of nociceptive TRPV1 responses.

EXPERIMENTAL PROCEDURES

Microplate Reader Measurement of Intracellular Ca^{2+} Responses in TRPV1/MOP HEK Cells—Double stable HEK293 cells expressing the μ opioid receptor (MOP) and TRPV1 (TRPV1/MOP HEK cells) were generated as described (12). TRPV1/MOP HEK cells were plated on PDL-coated 96-well plates and loaded with the fluorescent calcium probe Fluo-3-AM (6 μM) as described (12). Cells were washed 2–3 times with physiological salt solution (PSS; pH 7.4, composition KCl 5.9 mM, $MgCl_2$ 1.5 mM, NaH_2PO_4 1.2 mM, $NaHCO_3$ 5.0 mM, NaCl 140.0 mM, glucose 11.5 mM, $CaCl_2$ 1.8 mM, and HEPES 10.0 mM) and incubated for 15–30 min with pretreatments as appropriate. Preincubation steps and Ca^{2+} measurement were carried out at 29 °C to avoid dye sequestration.

Changes in fluorescence after addition of capsaicin were measured using a fluorescent multi-well plate reader (NOVOstar, BMG Labtechnologies, Victoria, Australia) with the excitation wavelength set at 485 nm and emission recorded at 520 nm. As previously described, calcium responses were represented as $\Delta F/F$ values (12). Maximum $\Delta F/F$ values were used to fit a 4-parameter logistic Hill equation to the data using GraphPad Prism (San Diego, CA, Version 4.03) to generate dose-response curves. All experiments were designed to include control experiments on the same plate as treated cells.

For calcium measurements using the $FLIPR^{TETRA}$ fluorometric imaging plate reader (Molecular Devices, Sunnyvale, CA), TRPV1/MOP HEK cells were plated on PDL-coated, black-walled 96-well plates (Corning, Lindfield, NSW, Australia). After loading with Fluo-3 AM (6 μM), cells were washed three times with PSS or nominal calcium-free PSS (composition: KCl 5.9 mM, $MgCl_2$ 1.5 mM, NaH_2PO_4 1.2 mM, $NaHCO_3$ 5.0 mM, NaCl 140.0 mM, glucose 11.5 mM, and HEPES 10.0 mM) as appropriate. Capsaicin and other reagents were injected from 3–4× concentrated stock solutions prepared in PSS or nominal calcium-free PSS with maximum final ethanol concentrations not exceeding 0.003%. Fluo-3-loaded cells were excited at 470–495 nm, and emission at 515–575 nm was recorded every second using a cooled CCD camera. For experiments requiring no extracellular calcium, BAPTA (final concentration 100 μM) was added 30 s prior to addition of capsaicin.

Whole Cell cAMP Accumulation Assay—TRPV1/MOP HEK cells were harvested with Versene (Invitrogen, Mount Waverley, Victoria, Australia) to avoid internalization of receptors. Cells were resuspended with anti-cAMP acceptor bead mix yielding final concentrations of 40,000 cells/well and 1 unit/well of anti-cAMP acceptor beads. Cells were incubated for 15–30 min with agonist in triplicate on 384-well plates (OptiPlate-384; PerkinElmer Life Sciences, Rowville, Victoria, Australia) and the reaction terminated by addition of lysis buffer containing Streptavidin Donor beads (1 unit/well) and biotinylated cAMP (1 unit/well). The plate was incubated under low light conditions for 16 h, and the bioluminescence reaction measured using the Envision Multilabel Plate Reader (PerkinElmer Life Sciences).

SDS-PAGE and Western Blotting—To assess monomeric and multimeric TRPV1 species, total cell protein was isolated and separated by SDS-PAGE essentially as previously described (13). Cells were grown to ~80% confluency and incubated for 25–30 min at 37 °C with the appropriate treatments in PSS. Cells were then immediately placed on ice, washed with ice-cold phosphate-buffered saline (PBS; composition in mM: NaCl 137, KCl 2.7, NaH_2PO_4 10, KH_2PO_4 1.8) and dislodged with ice-cold PBS. After centrifugation at 3,000 × *g* for 10 min, cells were resuspended in ice-cold PBS containing protease inhibitors (Roche Applied Science, Castle Hill, NSW, Australia) and sonicated briefly on ice. The supernatant was collected after centrifugation at 1,000 × *g* for 10 min at 4 °C and protein estimation carried out using the Bio-Rad protein estimation kit. Protein samples were analyzed on precast 4–20% iGel gradient gels without SDS (Life Therapeutics, Frenchs Forest, NSW, Australia). Total cell protein (20 μg) was mixed with 5× loading buffer (composition: 365 mM Tris-HCl, pH 6.8, 37.5% glycerol, 0.02% bromphenol blue, and 10% SDS to yield SDS end concentrations of 2%) and denatured at 65 °C for 10 min. Samples were separated at 150 V for ~60 min and transferred to nitrocellulose membrane for 1 h at 300 mA on ice in transfer buffer (composition: 25 mM Tris, 192 mM glycine, 15% methanol, pH 8.3). The nitrocellulose membrane was blocked overnight at 4 °C in blocking buffer (composition: 130 mM NaCl, 2.7 mM KCl, 10 mM NaH_2PO_4, 1.8 mM KH_2PO_4, 0.1% Tween-20, and 10% low-fat skim milk powder) and incubated for 1 h at room temperature with rabbit anti-rat TRPV1 antibody (1:5,000, Santa Cruz Biotechnology). A monoclonal anti-β-actin antibody (1:20,000, clone AC-15, Sigma Aldrich) was also included for visualization of β-actin to serve as a loading control. After washing in blocking buffer, the membrane was incubated for 1 h with anti-rabbit and anti-mouse horseradish peroxidase-conjugated secondary antibodies (both 1:5,000; Zymed Laboratories Inc., Mount Waverley, Victoria, Australia). Blots were developed using ECL Plus (GE Life Sciences, Rydalmere, NSW, Australia) for visualization of chemiluminescence by exposure to ECL Hyperfilm (GE Life Sciences). The optical density of bands was determined using MetaMorph Imaging Software (Version 6.2R5; Universal Imaging, Downington, PA).

[^{3}H]Resiniferatoxin Binding—For preparation of total cell membranes to assess binding of [^{3}H]resiniferatoxin to the TRPV1, cells were incubated at 37 °C in a 5% humidified CO_2 incubator with the appropriate treatment for 20–30 min, subsequently placed on ice, and washed 2–3 times with ice-cold PBS. Cells were dislodged with a cell scraper and collected by centrifugation at 3,000 × *g* for 5 min. The cells were resus-

pended in 1 ml of assay buffer (composition: 5 mM KCl, 5.8 mM NaCl, 2 mM $MgCl_2$, 320 mM sucrose, 10 mM HEPES; pH 7.4) and sonicated briefly. After centrifugation at 1,000 × *g* for 10 min, the supernatant was collected, and after protein estimation using a Bio-Rad protein assay kit, diluted to 20 μg of protein/200 μl with assay buffer containing an additional 0.25 mg/ml BSA.

Plasma membrane samples for [^{3}H]resiniferatoxin binding were prepared according to the manufacturer's instructions with a Plasma Membrane Protein Isolation kit (MBL International Corp, Woburn, MA) based on an aqueous two-phase polymer system of dextran-polyethylene glycol, which isolates plasma membrane proteins specifically with minimal contamination from other intracellular membrane fractions (14, 15) (supplemental Fig. S1). TRPV1/MOP HEK cells were incubated with the appropriate treatments in PSS at 37 °C for 20–30 min. Cells were placed on ice immediately, washed with ice-cold PBS, and 5–10 × 10^7 cells collected by centrifugation. The cell pellet was resuspended with 1 ml of the homogenization buffer included in the kit and briefly sonicated. The resulting homogenate was centrifuged at 700 × *g* for 10 min at 4 °C, and the resulting supernatant collected for protein estimation. For each treatment group, an identical amount of supernatant protein was utilized to isolate purified plasma membrane fractions. The plasma membrane protein pellet was collected by centrifugation at 44,800 × *g* for 30 min at 4 °C and resuspended in PBS for protein estimation. For [^{3}H]resiniferatoxin binding to the TRPV1, the plasma membrane protein was diluted to 5 μg of plasma membrane protein/200 μl with assay buffer containing 0.25 mg/ml BSA and used fresh.

Quantification of TRPV1 binding was performed by homologous competitive binding (16–19) in the presence of 50 pM [^{3}H]resiniferatoxin (PerkinElmer Life Sciences, 39.8 Ci/mmol) and varying concentrations of unlabeled resiniferatoxin. Nonspecific binding was defined as occurring in the presence of 1 μM non-radioactive resiniferatoxin. For total cell binding, 20 μg of protein was used, while for plasma membrane binding, 5 μg of purified plasma membrane fractions were sufficient. Using this protocol, nonspecific binding was generally below 10–20%, as previously reported (18). Binding reactions were carried out by incubation at 37 °C for 1 h and terminated by placing the assay mixtures on ice. Bound and free fractions were separated with a cell harvester on Whatman GF/B filters that had been soaked in filter buffer (composition: 50 mM Tris-HCl, 0.1% BSA, 0.5% polyethyleneimine; pH 7.4) at 4 °C for at least 1 h. Samples were read on a liquid scintillation counter after incubation of the filter papers with ~3 ml of liquid scintillant (OptiPhase HiSafe 3, PerkinElmer Life Sciences) at room temperature for 10–14 h. The analysis of radioligand binding data was performed using GraphPad Prism homologous competitive binding analysis with one class of binding sites.

Determination of Cell Viability by MTS Assay—The viability of TRPV1/MOP HEK cells was determined using the CellTiter 96® Aqueous One Solution Cell Proliferation Assay (Promega, Annandale, NSW, Australia) according to the manufacturer's specifications. In brief, cells were grown to ~80–90% confluency on 96-well plates and treated with varying concentrations of dansylcadaverine in PSS for 30 min. After a wash with PSS, cells were incubated with the MTS reagent for another 2 h at 37 °C in 5% CO_2 and absorbance measured at 490 nm with a Bio-Rad model 550 microplate reader.

Fluorescence Resonance Energy Transfer (FRET) Measurements—FRET signals from murine homomultimeric TRPV1 channels were determined as previously described (20). In brief, HEK293 cells were transiently transfected with a C-terminal Cerulean fluorescence protein-tagged TRPV1 construct (TRPV1-CFP) and a C-terminal enhanced yellow fluorescence protein-tagged TRPV1 construct (TRPV1-YFP) using Lipofectamine 2000 (Invitrogen). Fluorescence imaging was carried out at room temperature 1–2 days after transfection using a fully automated inverted fluorescence microscope (Olympus IX-81). For spectroscopic FRET measurements from the plasma membrane, a spectrograph (Acton SpectraPro 2150i) was used in conjunction with a Hamamatsu HQ CCD camera. Spectroscopic emission data specifically from the plasma membrane or the cytoplasm was collected by recording fluorescence intensity from the spectrograph slit location corresponding to each cellular structure as previously described (21). FRET efficiency was plotted as a function of the Cerulean to YFP fluorescence intensity ratio (Fc/Fy). Best fit FRET models were fitted to the data as previously described (20) and were represented as solid or dotted lines.

Immunofluorescence—TRPV1/MOP HEK cells were plated on 25-mm PDL-coated glass coverslips and grown to ~80–90% confluence. Cells were treated for 30 min at 37 °C with the appropriate reagents in PSS and placed immediately on ice to minimize receptor internalization. Cells were washed twice in ice-cold PBS before a light fix with methanol/acetone (1:1) at −20 °C for 30 min. After permeabilization with 0.2% Triton X in PBS for 10 min, cells were blocked by immersion in PBS with 3% BSA for 30 min. Rabbit anti-rat TRPV1 primary antibody (1:100, Santa Cruz Biotechnology) was prepared in PBS containing 3% BSA. After 1 h of incubation at room temperature, cells were incubated with anti-rabbit fluorescein isothiocyanate-conjugated secondary antibody (1:300) under low light for 1 h. Cells were mounted using SlowFade AntiFade (Molecular Probes). Randomly selected images were viewed on a Nikon Eclipse TE 300 inverted fluorescent microscope (excitation 488 nm, emission 520 nm) and recorded with MetaFluor (Molecular Devices) imaging software. Corel Photo-Paint (Corel, Ottawa, Ontario, Canada) was used for processing of images.

TRPV1 Expression in Calcium-rich Stores—As previously described (22), to assess TRPV1 expression in calcium-rich stores, the low affinity calcium probe Fura-FF was sequestered into intracellular stores by loading TRPV1/MOP HEK cells with Fura-FF-AM (12 μM) for 2 h at 37 °C, followed by washing with PSS for 15 min at 37 °C. Coverslips were transferred to the recording chamber of an inverted Nikon Eclipse TE 300 fluorescent microscope and viewed under a Nikon 40×/1.3 oil immersion objective lens. Fluorescence signals from single cells were ratio-imaged by recording emission intensity at 510 nm from excitation at 340 and 380 nm. Ratios of F340/F380 were depicted as pseudocolor images. Cells were then lightly fixed with 4% paraformaldehyde for 20 min and stained for TRPV1 expression as described above.

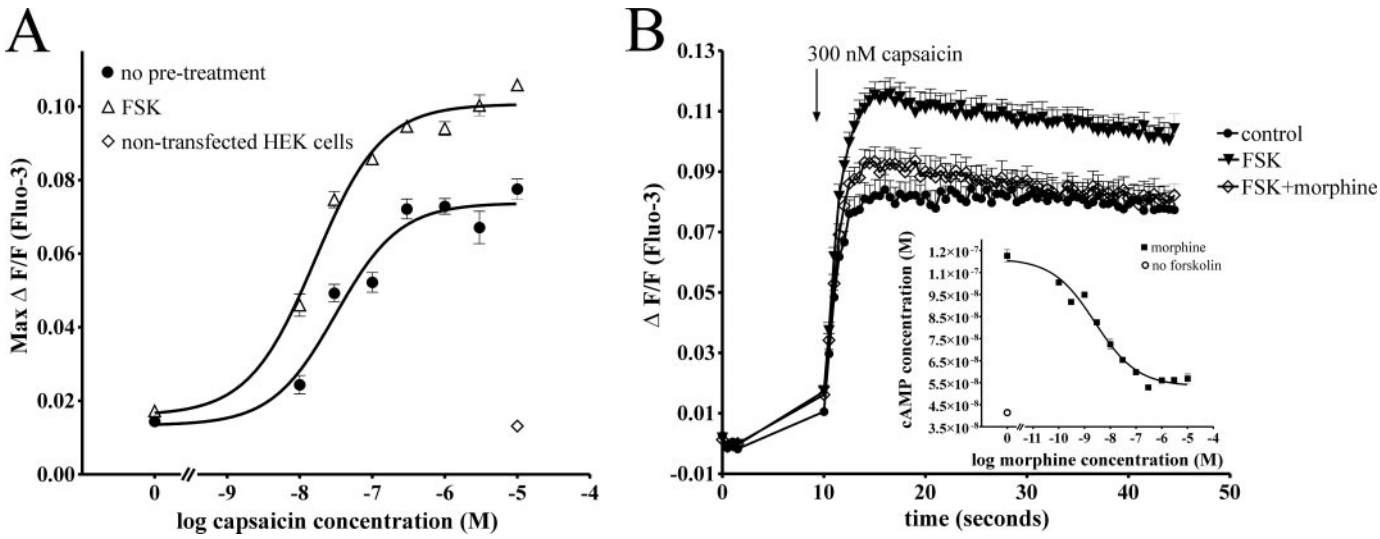

FIGURE 1. **TRPV1-mediated capsaicin responses are potentiated by cAMP-dependent PKA.** *A*, TRPV1/MOP HEK cells were treated with the PKA activator forskolin (Δ, FSK 50 μM) or PSS (●, no pretreatment), and calcium responses to the addition of capsaicin were monitored. Treatment with forskolin significantly ($p < 0.05$) increased TRPV1-mediated calcium responses over the entire capsaicin concentration range. Addition of capsaicin (10 μM) to non-transfected HEK cells did not lead to an increase in intracellular Ca^{2+} (◇, non-transfected HEK cells). *B*, *inset*, inhibition of forskolin-stimulated cAMP accumulation by morphine was assessed using an AlphaScreen cAMP assay. Treatment of TRPV1/MOP HEK cells with forskolin (50 μM) increased cAMP levels compared with untreated cells (○, no forskolin). Morphine dose-dependently inhibited cAMP accumulation stimulated by forskolin (50 μM) with a maximum effect at ~1 μM morphine. *B*, calcium responses to addition of 300 nM capsaicin were assessed in cells loaded with the fluorescent calcium probe Fluo-3. Cells were treated with PSS (●, *control*), forskolin (50 μM, ▼, *FSK*), or forskolin and morphine (1 μM, ◇, *FSK+morphine*) as required. Pretreatment of forskolin-stimulated TRPV1/MOP HEK cells with morphine (◇) significantly (*, $p < 0.05$) inhibited capsaicin-elicited calcium responses compared with cells treated with forskolin alone.

Assessment of TRPV1 Multimers and Immunofluorescence in DRG from Animals with Peripheral Inflammation—Ethical approval was obtained from the University of Queensland Animal Ethics Committee and experiments carried out in accordance with guidelines of the Committee for Research and Ethical Issues of the International Association for the Study of Pain. Adult male Wistar rats (250–300 g) were kept in a controlled environment at a temperature of 22 ± 0.5 °C, relative humidity of 40–60%, and a 12 h (6:30 AM to 6:30 PM) light-dark cycle with free access to standard lab chow and tap water. To induce peripheral inflammation, 100 μl of Freund's Complete Adjuvant (FCA, Sigma) was injected subcutaneously into the right hind paw under light isoflurane anesthesia. L5 DRGs ipsilateral to the inflamed paw were isolated 6–7 days after induction of inflammation. For analysis of TRPV1 multimerization in DRG neurons, individual L5 DRG were placed immediately in ice-cold PBS containing protease inhibitors (Roche Applied Sciences), minced with surgical scissors and sonicated on ice. Protein samples were collected after centrifugation at 1,000 × *g* for 10 min and 20 μg of protein analyzed by SDS-PAGE and Western blotting as described above.

For immunofluorescence studies of plasma membrane TRPV1 expression, L5 DRG contralateral and ipsilateral to the inflamed paw were harvested and immediately fixed for 2–3 h in ice-cold paraformaldehyde (4%). DRGs were then transferred to 0.32 M sucrose and cryoprotected at 4 °C for at least 24 h. Tissues were embedded in Tissue-Tek® O.C.T. Compound (Sakura Finetek, Torrance, CA), cut to 10-μm cryostat sections, and mounted on SuperFrost Ultra Plus® tissue adhesion slides (Menzel GmbH Co KG, Braunschweig, Germany) before immunofluorescence labeling as described above.

Data Analysis—Unless otherwise states, all graphs are representative of at least two to three independent experiments with minimum *n* values for each treatment group being $n = 3$. Unless individual data points are shown, data are presented as means ± S.E. of the mean (S.E.). As mentioned above, statistical analysis and fitting of 4-parameter Hill equations were carried out using GraphPad Prism Version 4.03. Statistical significance was defined as $p < 0.05$ and determined using an unpaired, two-tailed Student's *t* test where appropriate. Calcium traces were analyzed by statistical comparison of maximum ΔF/F values using an unpaired, two-tailed Student's *t* test with statistical significance defined as $p < 0.05$.

RESULTS

Capsaicin Responses Potentiated by cAMP-dependent PKA Are Inhibited by Morphine—Potentiation of TRPV1-mediated Ca^{2+} responses to addition of varying concentrations of capsaicin was assessed after a short (15 min) incubation with 0.1% DMSO (control) or forskolin (50 μM, Fig. 1*A*). Treatment with the adenylate cyclase activator forskolin leads to an increase in cellular cAMP levels and resultant activation of cAMP-dependent PKA. PKA-mediated phosphorylation of TRPV1 in turn causes sensitization of TRPV1 responses (23). While cAMP analogues acting directly at PKA lead to a similar sensitization, opioids, by virtue of their antihyperalgesic activity resulting from adenylate cyclase inhibition, are unable to prevent TRPV1 sensitization by direct PKA activators (12). Thus, to assess the opioid-sensitive mechanisms involved in TRPV1 sensitization by cAMP-dependent PKA, forskolin was used to potentiate TRPV1 responses. Consistent with previously described studies (12), treatment with forskolin significantly increased TRPV1-mediated capsaicin responses (Fig. 1, *A* and *B*, $p < 0.001$). The (MOP) agonist morphine inhibited this potentiation (Fig. 1*B*) through inhibition of forskolin-stimulated cAMP production, which was maximal at 1 μM morphine, although reversal of

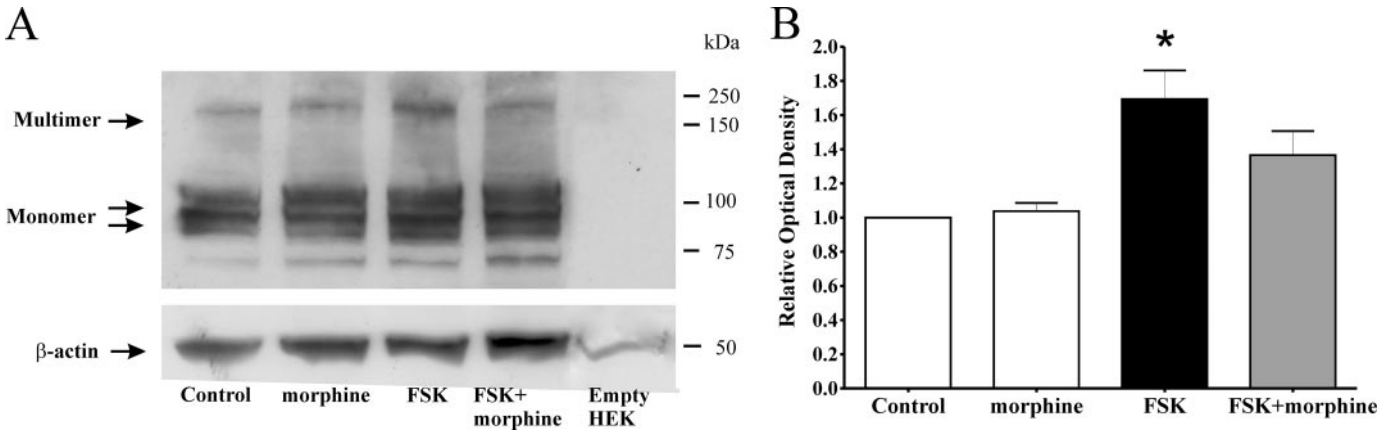

FIGURE 2. **Activation of cAMP-dependent PKA by forskolin increases total cell TRPV1 multimerization.** *A*, Western blot of TRPV1/MOP HEK cell protein from cells treated with 0.1% DMSO (*Control*), morphine (1 μM) and forskolin (*FSK*, 500 μM) in the absence or presence of morphine (1 μM, *FSK+morphine*). Non-transfected HEK cells were used as a control, with size markers in kDa shown on the *right*. Total cell lysates were prepared under non-reducing conditions and analyzed by SDS-PAGE on 4–20% precast gradient gels. Similar results were obtained in four independent experiments. *B*, optical density of TRPV1 multimer bands were obtained using MetaMorph (Molecular Devices), normalized to β-actin and expressed relative to control. Treatment with forskolin (*FSK*, *black bar*) significantly (*, $p < 0.05$ compared with control by ANOVA) increased TRPV1 multimer density in total cell lysates.

forskolin-stimulated cAMP accumulation by morphine was not complete (Fig. 1*B*, *inset*). We then focused on assessing the mechanism of potentiation of TRPV1 by forskolin.

Treatment of TRPV1/MOP HEK Cells with the PKA Activator Forskolin Increases TRPV1 Multimerization—Augmentation of TRPV1 responses by forskolin (Fig. 1*A*) appears consistent with an increase in functional TRPV1 channels. However, it is unclear how forskolin could achieve an increase in functional TRPV1 channels in a way that would be consistent with rapid and dynamic regulation of nociceptive TRPV1 signaling. As functional TRPV1 channels are proposed to exist in homomultimeric form (14, 19–23), one mechanism for cAMP-mediated promotion of TRPV1 responses is assembly of pre-existing plasma membrane TRPV1 monomers to form new functional plasma membrane multimeric TRPV1 channels.

We assessed total cell TRPV1 multimerization by SDS-PAGE under non-reducing conditions, as described previously (13, 24). TRPV1 monomers and multimers are detectable by SDS-PAGE under non-reducing conditions (13). Indeed, we observed bands consistent with glycosylated and unglycosylated TRPV1 monomers (97 and 113 kDa, respectively) as well as a multimeric TRPV1 species (~200 kDa) under these conditions (Fig. 2*A*). This multimeric species represents a TRPV1 dimer, which is particularly stable, has previously been demonstrated to parallel formation of the less stable tetramer, and can be used to assess oligomerization of TRPV1 (13, 25).

TRPV1/MOP HEK cells were treated with 0.1% DMSO (control), morphine (1 μM), or forskolin (500 μM, FSK) containing in addition morphine (FSK+morphine) as appropriate (Fig. 2, *A* and *B*). Treatment with forskolin significantly ($p < 0.05$ by ANOVA) increased TRPV1 multimer formation, while pretreatment with morphine reversed this increase (Fig. 2, *A* and *B*).

Treatment with the Transglutaminase Inhibitor Dansylcadaverine Inhibits Capsaicin Responses Potentiated by Forskolin—To determine if TRPV1 functionality is affected when TRPV1 multimers are disrupted, we preincubated TRPV1/MOP HEK cells with varying concentrations of the transglutaminase inhibitor dansylcadaverine and assessed calcium responses to the addition of 300 nM capsaicin in control and forskolin-stimulated cells (Fig. 3*A*). Preincubation with dansylcadaverine at previously reported concentrations (26) inhibited capsaicin responses in control and forskolin-treated cells, consistent with the functional form of the TRPV1 as a multimer (14, 20–23). Forskolin-treated cells were more sensitive to dansylcadaverine ($\log EC_{50\ (Control)} -3.185 \pm 0.027$; $\log EC_{50\ FSK} -3.269 \pm 0.013$; $p < 0.05$). The inhibition of capsaicin responses by dansylcadaverine was not due to impaired cell viability, globally impaired calcium responses, or TRPV1 antagonism (Fig. 3, *B–D*). There was no displacement of the radiolabeled TRPV1 agonist [^{3}H]resiniferatoxin by unlabeled dansylcadaverine (100 μM to 1.2 mM), indicating that the transglutaminase inhibitor does not act as a competitive TRPV1 antagonist (Fig. 3*B*). Preincubation with dansylcadaverine did not affect responses to the calcium ionophore ionomycin (10 μM, Fig. 3*C*), or cell viability over this period (Fig. 3*D*). Inhibition of forskolin-stimulated capsaicin responses by dansylcadaverine appears to be a consequence of inhibition of functional TRPV1 multimer formation.

Forskolin Does Not Increase Multimerization of TRPV1 Monomers in the Plasma Membrane—Last, to assess the effect of forskolin on changes in the proportion of plasma membrane TRPV1 multimers and monomers, we quantified TRPV1 multimerization utilizing a well characterized spectroscopy FRET model (20) that allows quantification of FRET signals specifically from the plasma membrane. HEK cells were transiently transfected with Cerulean fluorescence protein-tagged TRPV1 (TRPV1-CFP) and enhanced yellow fluorescence protein-tagged TRPV1 (TRPV1-YFP) and the FRET signal determined as previously described (20) prior to and after treatment with forskolin (500 μM). No increase in FRET signal, a measure of *de novo* formation of TRPV1 multimers from pre-existing plasma membrane monomers, was detected (Fig. 4). Hence, increases in cellular cAMP do not cause multimerization of TRPV1 monomers in the plasma membrane; rather, our results are

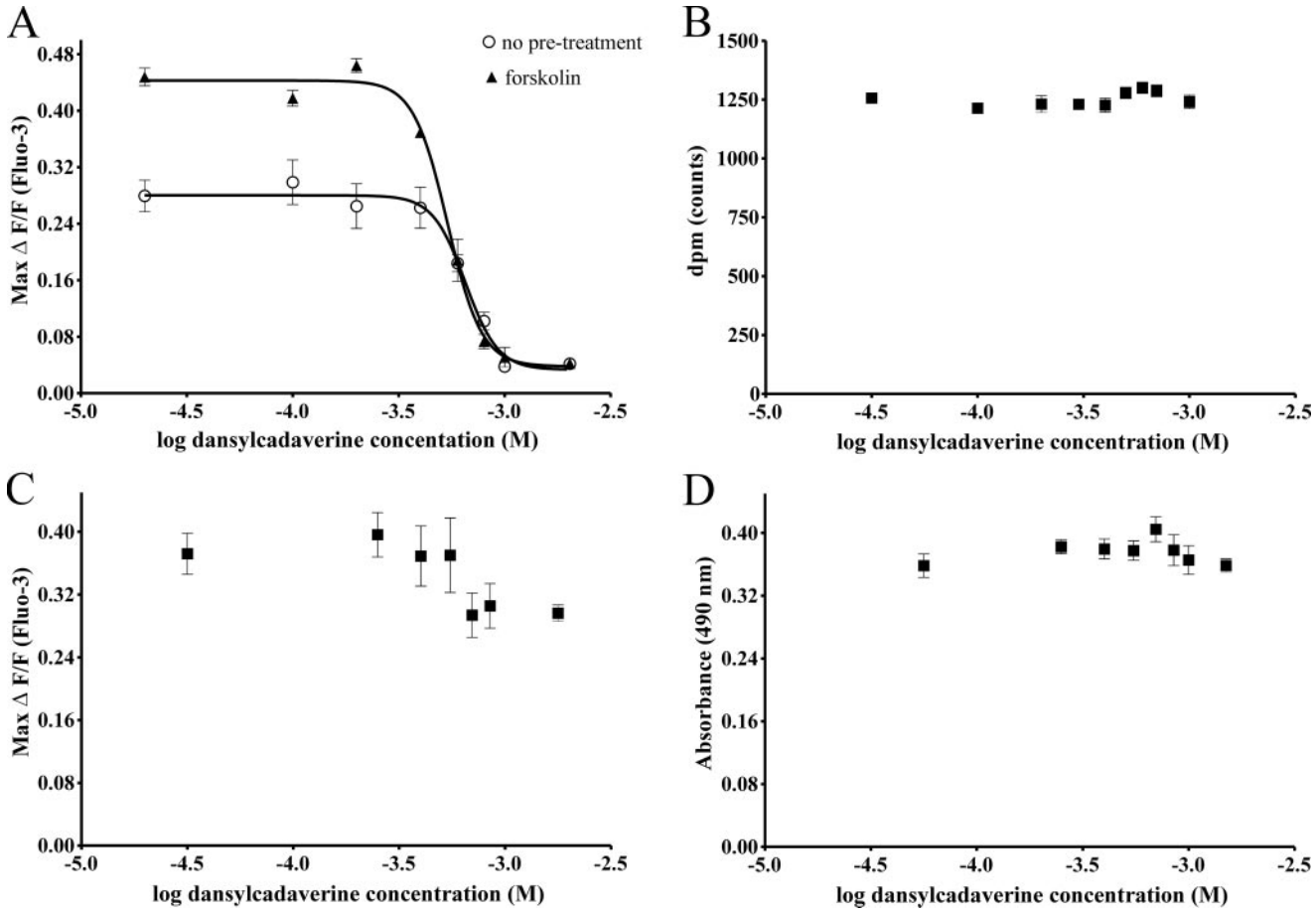

FIGURE 3. **Dansylcadaverine inhibits TRPV1-mediated capsaicin responses potentiated by Forskolin.** *A*, TRPV1/MOP HEK cells were treated with 0.1% DMSO (control, ○) or forskolin (500 μM, FSK, ▲) and calcium responses to addition of 300 nM capsaicin monitored in the presence of varying concentrations of the transglutaminase inhibitor dansylcadaverine. Treatment with dansylcadaverine significantly inhibited ($p < 0.01$ by ANOVA with Tukey's postcomparison) basal and forskolin-potentiated capsaicin responses. *B*, displacement of [^{3}H]resiniferatoxin binding to TRPV1 by dansylcadaverine was assessed by exposing TRPV1/MOP HEK total cell lysates to 50 pM [^{3}H]resiniferatoxin in the presence of varying concentrations of unlabeled dansylcadaverine. Dansylcadaverine does not act as a TRPV1 receptor antagonist, as [^{3}H]resiniferatoxin binding was not affected by dansylcadaverine ($p > 0.05$ by ANOVA). *C*, TRPV1/MOP HEK cells were treated with varying concentrations of dansylcadaverine for 30 min and calcium responses to the addition of ionomycin (10 μM) was assessed using Fluo-3. Treatment with dansylcadaverine did not significantly inhibit ionomycin responses ($p > 0.05$ by ANOVA) even at concentrations that completely abolished capsaicin responses. *D*, cell viability after treatment with dansylcadaverine was determined using an MTS assay. TRPV1/MOP HEK cells were treated with varying concentrations of dansylcadaverine for 30 min, and the number of viable cells determined by measuring absorbance at 490 nm. Treatment with dansylcadaverine did not adversely affect cell viability ($p > 0.05$ by ANOVA). Results are representative of 2–3 independent experiments with $n = 4–8$ per treatment.

consistent with a model whereby forskolin increases plasmalemmal TRPV1 multimers from an internal pool of monomers.

TRPV1 Multimers Are Mainly Localized to the Plasma Membrane—To determine if the intracellular pool of TRPV1 available for plasma membrane insertion was indeed in a multimeric or monomeric state, we compared the relative proportion of TRPV1 multimers and monomers in intracellular pools and the plasma membrane. If forskolin was to promote the assembly and rapid translocation of newly formed TRPV1 multimers to the plasma membrane from a pool of intracellular TRPV1 monomers, the majority of TRPV1 monomers would be found intracellularly, with a correspondingly large proportion of TRPV1 multimers existing on the plasma membrane. Assessment of the FRET signal from the plasma membrane and intracellular compartments clearly demonstrated that TRPV1 multimers occur mainly on the plasma membrane, while the correspondingly lower FRET signal from intracellular compartments is consistent with a higher proportion of TRPV1 monomers (Fig. 5*A*). To assess the functionality of TRPV1 in these internal pools, we determined the presence of TRPV1 on calcium-rich intracellular compartments and monitored calcium release from stores in response to capsaicin. The low affinity ratiometric calcium dye Fura-FF-AM (12 μM) was sequestered into intracellular stores. High Fura-FF fluorescence ratios (F340/F380) indicative of high calcium levels were found in similar patterns to TRPV1 immunofluorescence (Fig. 5*B*). Although the TRPV1 was clearly expressed in calcium-rich intracellular compartments, addition of capsaicin did not increase cytosolic free calcium levels in the absence of extracellular calcium (Fig. 5*C*). This is consistent with an intracellular pool of inactive monomeric TRPV1 being available for plasma membrane insertion, where it exists in a multimeric state.

Augmentation of TRPV1 Activity Is Associated with TRPV1 Translocation to the Plasma Membrane—Translocation of TRPV1 channels to the plasma membrane was assessed in TRPV1/MOP HEK cells treated with 0.1% DMSO (control), forskolin (500 μM, FSK), or morphine with forskolin (1 μM, FSK+morphine). As predicted by our model, treatment with

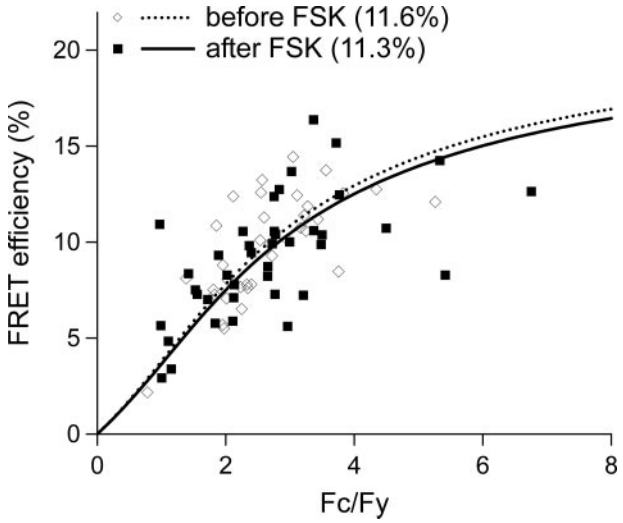

FIGURE 4. **Treatment with forskolin does not affect TRPV1 monomer to multimer ratio in plasma membrane.** HEK cells were transiently transfected with TRPV1-CFP and TRPV1-YFP and FRET efficiency measured from the plasma membrane of cells before (◇, *dotted line*) and after (■, *solid line*) treatment with 500 μM forskolin. Treatment with forskolin did not affect the total plasma membrane FRET signal, indicating no change in the ratio of TRPV1 monomers to TRPV1 multimers in the plasma membrane. Each point represents measurements from a single cell.

forskolin caused a marked translocation of TRPV1 immunoreactivity to the plasma membrane (Fig. 6*A*), resulting in distinct membrane labeling. Pretreatment with morphine inhibited the predominant plasma membrane TRPV1 expression pattern and reversed TRPV1 labeling to mixed plasma membrane and cytoplasmic localization (Fig. 6*A*). To exclude the possibility that treatment with forskolin could increase *de novo* synthesis of TRPV1 channels on the plasma membrane, we further assessed TRPV1 binding density in isolated plasma membrane protein fractions and total cell protein (Fig. 6, *B* and *C*) using homologous competitive binding analysis.

Plasma membrane TRPV1 radioligand binding density in TRPV1/MOP HEK cells treated with forskolin (500 μM, FSK) was significantly increased ($p < 0.05$, B_{max} FSK, 1284.6 ± 419.2 pmol/mg protein) compared with control (Fig. 6*B*, B_{max} control, 685.1 ± 310 pmol/mg protein). In agreement with our immunofluorescence studies, pretreatment with morphine reversed this increased plasma membrane binding density (B_{max} FSK+morphine, 331.3 ± 156.1 pmol/mg protein; Fig. 6*B*). Consistent with our model, total cell [^{3}H]resiniferatoxin binding was unaffected by treatment with forskolin or morphine (Fig. 6*C*, $p > 0.05$), indicating that the increase in plasma membrane TRPV1 expression was due to translocation of TRPV1 channels rather than increased formation of new TRPV1 protein.

TRPV1 Multimers and Plasma Membrane Expression in Inflammation—We assessed whether two pools of TRPV1 (multimers and monomers) are present *in vivo* during inflammation, a process where signaling through cAMP-dependent PKA is increased (27). Western blot analysis demonstrated that, as previously suggested, TRPV1 protein was present in inflamed DRG in two distinct pools representing monomeric and multimeric species (Fig. 7*A*). The presence of monomeric and multimeric TRPV1 provides the basis for rapid dynamic regulation of TRPV1 responses via the mechanisms we propose in addition to increased TRPV1 expression in inflammation (28–31). Contribution of these pathways to *in vivo* TRPV1 sensitization is also suggested by the increased TRPV1 plasma membrane staining patterns in L5 DRG ipsilateral to the inflamed hind paw (Fig. 7*B*).

DISCUSSION

Potentiation of TRPV1 responses by cAMP-dependent PKA is crucial to the development of inflammatory hyperalgesia. Although PKA consensus sites for TRPV1 have been identified (32, 33), the molecular pathways leading to the rapid sensitization of the receptor as a result of PKA-mediated phosphorylation are not fully understood. Our results propose a newmechanismdescribinghowTRPV1potentiationbycAMP-dependent PKA can be achieved rapidly without the need for translational changes, while maintaining the capacity for dynamic modulation of sensitized TRPV1 signaling. Our results propose a mechanism for potentiation of TRPV1 responses by cAMP-dependent PKA incorporating both increased TRPV1 translocation and multimerization (Fig. 8). The dynamic regulation of these pathways by opioids represents a cellular mechanism allowing for rapid modification of the hyperalgesic or sensitized component of TRPV1 signaling.

The TRPV1 is a target for inflammatory signaling through cAMP-dependent PKA. As an activator of adenylate cyclase causing elevation of cellular cAMP levels, forskolin affects potentiation of TRPV1 responses as a result of activation of cAMP-dependent PKA (2, 23). Potentiation of TRPV1-mediated capsaicin responses by forskolin is consistent with an increase in functional TRPV1 channels and indeed, increased TRPV1 expression occurs in inflammation (29, 31). However, as the potentiation of capsaicin responses by forskolin occurs rapidly, pathways other than increased transcription of TRPV1 must be involved and were assessed in this study.

The functional TRPV1 channel exists most likely as homomultimers, whereby monomeric TRPV1 subunits assemble in tetrameric stoichiometry around the aqueous pore (13, 34). The most compelling confirmation of the functional importance of correct assembly of TRPV1 subunits arguably arises from the observation that incorporation of a single dominant negative mutant into the TRPV1 channel complex completely abolishes capsaicin responses (34). Surprisingly, despite clear evidence that TRPV1 multimerization is essential for channel function, regulation of multimerization has not been described as a possible contributor to post-translational modification of TRPV1 function. An increase in TRPV1 multimerization would provide a cellular mechanism for achieving rapid modulation of TRPV1 signaling without the need for altered transcription. Indeed, we found that treatment with forskolin significantly increased TRPV1 multimers in total cell lysates, indicating that the rapid potentiation of TRPV1 responses after treatment with forskolin might involve the generation of new functional units of TRPV1. Pretreatment with morphine prevented a significant increase in TRPV1 multimerization, providing evidence that this system could present a pathway for rapid and dynamic modulation of TRPV1 potentiation.

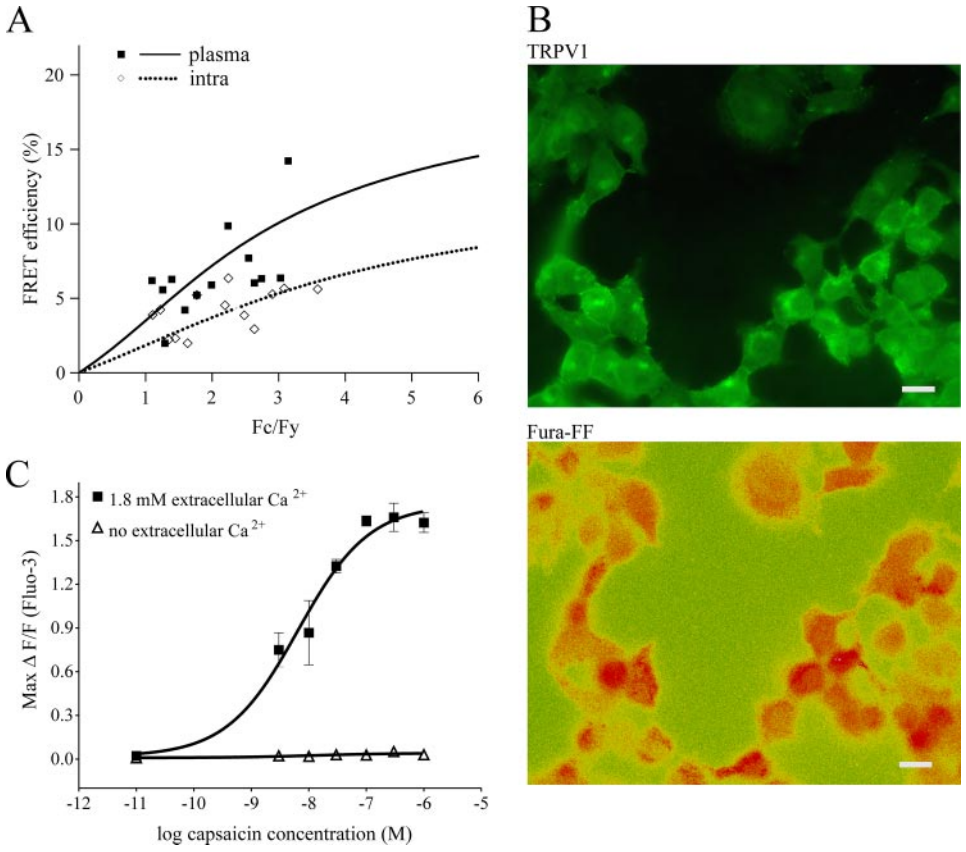

FIGURE 5. **Functional TRPV1 multimers are located in the plasma membrane.** *A*, FRET efficiency from the plasma membrane and intracellular structures was determined in HEK cells transfected with TRPV1-CFP and TRPV1-YFP. TRPV1 multimers, as assessed by FRET efficiency from plasma membrane, were increased in the plasma membrane compared with intracellular structures. Each point represents measurements from a single cell with the same cell quantified for both intracellular (◇, *dotted line*, intra) and plasma membrane (■, *solid line*, plasma) fluorescence. *B*, expression of TRPV1 on calcium-rich intracellular compartments was determined by loading cells with the fluorescent calcium dye Fura-FF-AM. TRPV1 immunofluorescence (*green*, *TRPV1*) was found in similar patterns to high Fura-FF emission ratios (*red*, *Fura-FF*, F340/F380) indicative of high calcium levels. *Scale bar*, 20 μm. *C*, functionality of intracellular TRPV1 channels was assessed by monitoring capsaicin-induced calcium responses in nominal calcium-free medium after addition of the calcium chelator BAPTA (100 μM). Although TRPV1 was clearly expressed in calcium-rich intracellular compartments, addition of capsaicin did not elicit an increase in intracellular calcium in the absence of extracellular calcium (△), in contrast to capsaicin-elicited responses in the presence of 1.8 mM extracellular calcium (■).

Activation of adenylate cyclase can increase transglutaminase activity and expression (32, 33), and TRPV1 cross-linking has previously been demonstrated to involve transglutaminases (13). Thus, we assessed the ability of forskolin to potentiate TRPV1-mediated capsaicin responses under conditions where TRPV1 multimers are disrupted. In accordance with increased TRPV1 multimerization in response to forskolin, capsaicin responses were sensitive to the transglutaminase inhibitor dansylcadaverine, demonstrating the importance of functional TRPV1 multimers in mediating TRPV1 potentiation by forskolin.

To assess the effect of forskolin on changes in the proportion of plasma membrane TRPV1 multimers and monomers, we quantified TRPV1 multimerization by FRET. Increased multimerization of TRPV1 monomers in a mixed population of plasma membrane TRPV1 subunits would result in an increase in FRET. The FRET signal from the plasma membrane was not affected by forskolin, indicating that the increase in TRPV1 multimers did not result from an increase in cross-linking of pre-existing monomers in the plasma membrane. As FRET is not affected by absolute fluorescence intensity and thus insensitive to insertion of preformed multimers into the plasma membrane, this would suggest that rather than promoting multimerization of TRPV1 monomers in the plasma membrane, forskolin might affect insertion of TRPV1 multimers into the plasma membrane. However, simple translocation of functional TRPV1 multimers preformed in intracellular stores would not only be inconsistent with an overall increase in TRPV1 multimerization, but in addition would likely lead to major alteration of calcium homeostasis in intracellular stores. An intracellular store of inactive TRPV1 monomers, however, would provide a source of TRPV1 subunits available for translocation to the plasma membrane that would not produce major disruptions in calcium homeostasis. These monomers are likely to be translocated to the plasma membrane, where they become inserted as functional TRPV1 multimers, thus providing a physiological mechanism for rapid assembly of functional TRPV1 units. Consistent with this model, the plasma membrane would be expected to contain significantly more TRPV1 multimers than the intracellular space. This was indeed shown to be the case, as evaluation of the FRET signals from intracellular and plasma membrane regions revealed that TRPV1 multimers are more abundant in the plasma membrane than in intracellular regions.

Further functional evidence supporting our proposed model stems from the observation that TRPV1 does not mediate significant calcium release from intracellular stores at concentrations that cause considerable influx of calcium through the plasma membrane. Several studies report TRPV1 expression in intracellular structures such as the endoplasmic reticulum, both in native as well as overexpressed cell systems (31–33), and TRPV1 expression in calcium-rich intracellular stores was confirmed here. If intracellular TRPV1 channels were indeed preassembled as functional channels, this should translate into effective release of calcium from intracellular stores upon channel activation, as TRPV1 agonists such as capsaicin are highly lipophilic and readily cross the cell membrane (35). While some studies have attributed calcium release channel properties to the TRPV1, calcium release from stores generally occurred at significantly higher capsaicin concentrations than those required to elicit calcium influx through plasma membrane

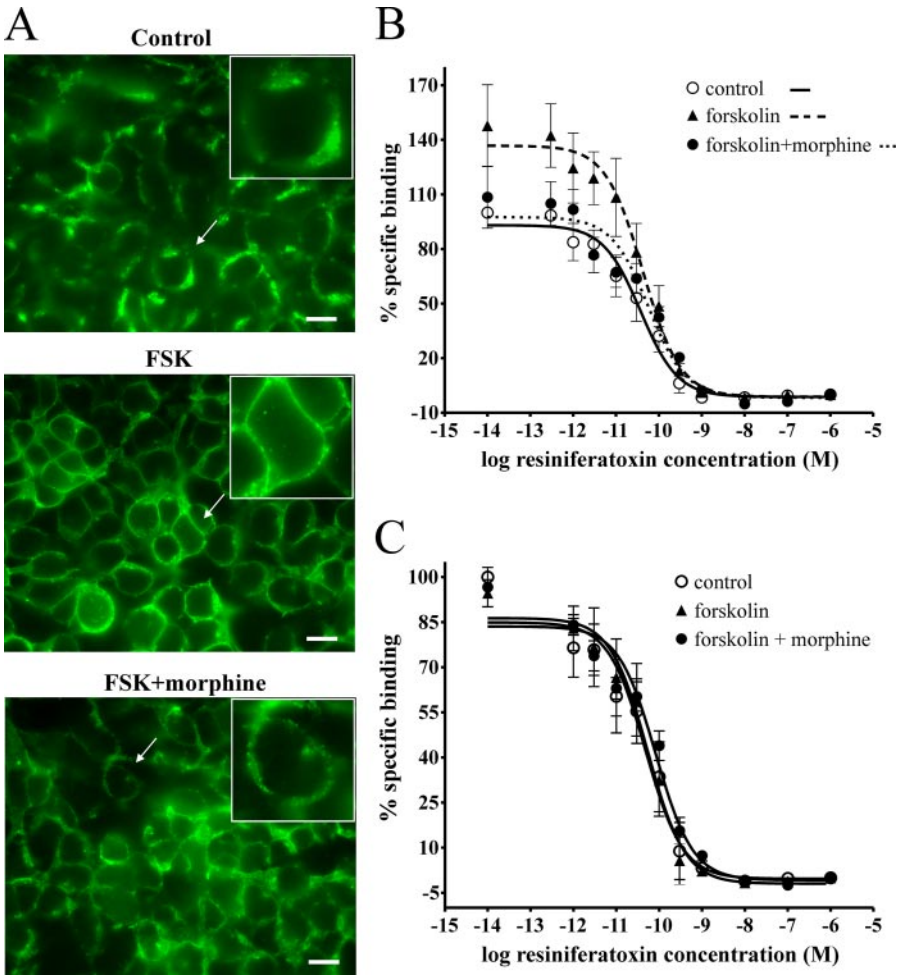

FIGURE 6. **Plasma membrane TRPV1 localization is increased by treatment with forskolin and reversed by morphine.** *A*, treatment with forskolin caused translocation of TRPV1 immunoreactivity to the plasma membrane. TRPV1/MOP HEK cells were treated with 0.1% DMSO (*Control*), forskolin (500 μM, *FSK*), or forskolin and morphine (1 μM, *FSK+morphine*) and stained for TRPV1 expression (*green*). Treatment with forskolin caused a marked shift in TRPV1 localization to plasma membrane-dominant expression (*FSK*). Pretreatment with morphine reversed TRPV1 staining to mixed plasma membrane and cytosolic pattern (*FSK+morphine*). *Scale bar*, 20 μm. Data are representative of three independent experiments. *A*, *inset*, magnified view (×1.6) of cells indicated by an *arrow*. *B*, plasma membrane TRPV1 binding density is increased by treatment with forskolin. Quantification of plasma membrane TRPV1 protein was assessed by [^{3}H]RTX binding to purified plasma membrane samples. TRPV1/MOP HEK cells were treated with 0.1% DMSO (*control*, ○) or forskolin (500 μM, ▲) containing in addition morphine (1 μM) as required (FSK+morphine, ●), and [^{3}H]resiniferatoxin displacement from purified plasma membrane preparations was assessed in the presence of various concentrations of unlabeled resiniferatoxin. Treatment with forskolin increased TRPV1 binding density in plasma membrane fractions compared with control, and this increase was reversed by pretreatment with morphine. Data are presented as mean ± S.E. from five independent experiments. *C*, total cell TRPV1 binding density is not affected by treatment with forskolin. [^{3}H]Resiniferatoxin displacement from total cell protein preparations was assessed in TRPV1/MOP HEK cells treated with 0.1% DMSO (*control*, ○) or forskolin (500 μM, ▲) containing in addition morphine (1 μM) as required (FSK+morphine, ●). Treatment with forskolin did not affect total cell TRPV1 binding density. Data are presented as mean ± S.E. from five independent experiments.

TRPV1 (31–33). Indeed, EC_{50} values of up to 13 μM are reported for capsaicin-mediated calcium release from intracellular stores (36), while the corresponding EC_{50} for calcium influx through plasma membrane TRPV1 is ~30–40 nM (12, 37). Because high capsaicin concentrations are associated with nonspecific effects including activation of phospholipase C (38), mechanisms other than TRPV1 activation likely contribute to the release of calcium from intracellular stores in response to high concentrations of capsaicin. Similarly, the TRPM8 agonist menthol appears to release calcium from the ER and Golgi via a TRPM8-independent mechanism (39). We systematically compared capsaicin dose response curves in the presence and absence of extracellular calcium and found that, consistent with a largely inactive pool of TRPV1 in intracellular structures, negligible store release occurs in response to capsaicin concentrations that cause significant calcium influx through the plasma membrane. Indeed, an intracellular reservoir of active TRPV1 channels could be detrimental to cellular calcium homeostasis given that TRPV1 agonists are generally lipophilic (35).

Promotion of TRPV1 multimerization from intracellular monomers by forskolin would require rapid translocation of these TRPV1 channels to the plasma membrane. Consistent with studies describing mixed intracellular and plasma membrane localization for TRPV1 in both native cells as well as overexpressed systems (22, 31, 32), control cells displayed significant expression of TRPV1 in intracellular structures, while some punctuate TRPV1 localization was apparent in the plasma membrane. In contrast, treatment with forskolin resulted in a striking shift in TRPV1 immunofluorescence to the plasma membrane, resulting in a distinct ring-like pattern. Pretreatment with morphine demonstrated that this translocation can be dynamically modulated, as the predominant plasma membrane localization of TRPV1 was largely lost. Increased TRPV1 translocation by forskolin and inhibition thereof by morphine was further confirmed by quantification of [^{3}H]resiniferatoxin binding to purified plasma membrane fractions. These findings demonstrate that the mechanisms underlying rapid potentiation of TRPV1-mediated capsaicin responses by the adenylate cyclase activator forskolin can be dynamically modulated by morphine, an observation that could be of particular relevance to inflammatory hyperalgesia. Such opioid-mediated modulation of TRPV1 multimerization and trafficking could, in addition to effects of opioids on other inflammatory mediators (40–46), also contribute to the enhanced anti-nociceptive effect of opioids in inflammation.

The exact pathways involved in trafficking and multimerization of TRPV1 by cAMP-dependent PKA remain to be elucidated. Notably, both PKA phosphorylation sites as well as putative SNARE interaction sites are located on the N-terminal of

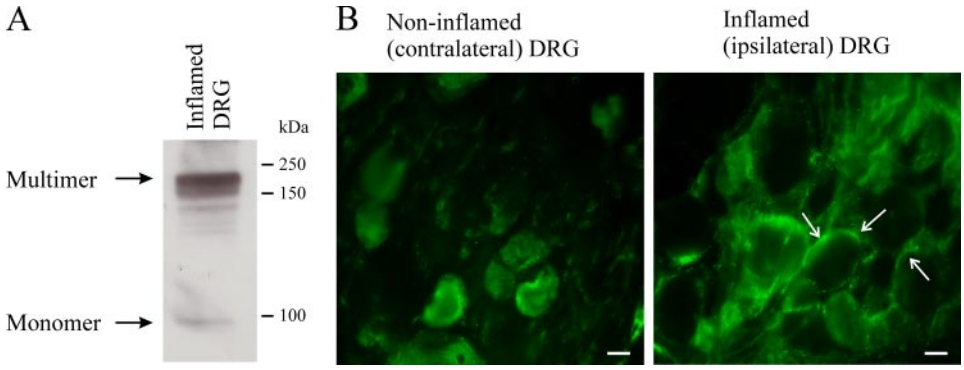

FIGURE 7. **TRPV1 expression in inflammation.** *A*, inflammation was induced in adult male Wistar rats by injection of Freund's Complete Adjuvant. Protein from L5 DRG ispsilateral to the inflamed paw was analyzed by SDS-PAGE. TRPV1 monomers and multimers occur in inflamed DRG, providing the basis for increased multimerization in inflammation. *B*, TRPV1 expression in L5 DRG ipsilateral and contralateral to the inflamed paw shows increased plasma membrane localization of TRPV1 in inflamed DRG compared with non-inflamed DRG. Data are representative of five animals with peripheral hind paw inflammation. *Arrows* point to TRPV1 immunofluorescence localized to the plasma membrane.

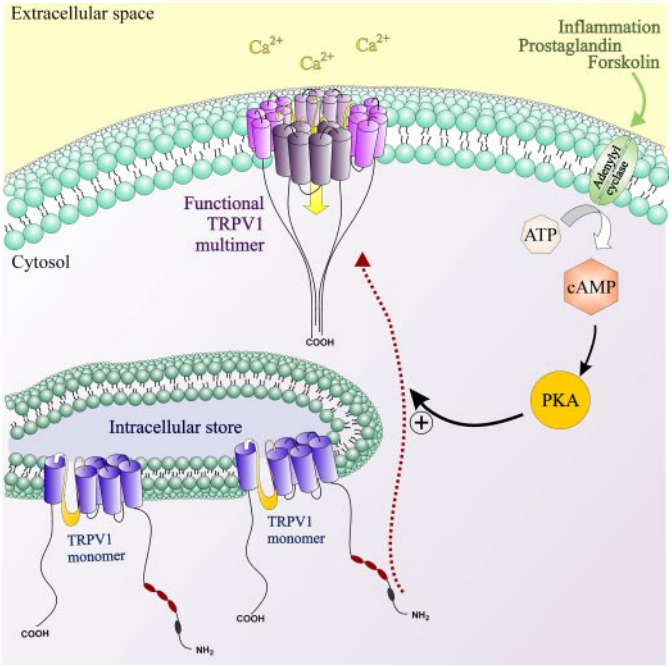

FIGURE 8. **Schematic representation of mechanisms involved in potentiation of TRPV1 responses by forskolin.** An intracellular pool of monomeric TRPV1 subunits becomes multimerized and inserted into the plasma membrane as functional TRPV1 multimers in response to activation of adenylate cyclase by forskolin. This increase in functional TRPV1 channels located on the plasma membrane translates to potentiation of TRPV1-mediated capsaicin responses by forskolin. Morphine, via inhibitory action on adenylate cyclase, can dynamically modulate TRPV1 multimerization and trafficking, thus resulting in inhibition of forskolin-stimulated TRPV1 responses. An intracellular store of TRPV1 monomers allows for rapid modulation of TRPV1 signaling independent of transcriptional changes without disruption to intracellular calcium homeostasis by effecting calcium store depletion.

TRPV1 (8, 47, 48), such that phosphorylation of TRPV1 by PKA could lead to enhancement of these exocytosis pathways through to-date unknown mechanisms. Indeed, PKA-dependent trafficking pathways have been reported for a number of receptors and ion channels including the chloride-selective anion channel CFTR and AMPA receptor (49, 50). Alternatively, increased multimerization and translocation of TRPV1 could occur as a downstream result of PKA-mediated phosphorylation of other effectors rather than as a direct result of phosphorylation of TRPV1 by PKA. Indeed, TRPV1 has been reported to bind to several proteins involved in receptor trafficking, including Snapin and synaptotagmin IX as well as eferin (48, 51). The function of these proteins in turn can be affected by PKA-mediated phosphorylation (52). As several other proteins have been reported to regulate trafficking of various trp channels (53), the exact pathways involved in PKA-mediated TRPV1 trafficking remain to be identified.

Similarly, in addition to increased transglutaminase activity and expression as a result of activation of adenylate cyclase (32, 33), other pathways not implicated to date may be involved in increased multimerization of TRPV1 by cAMP-dependent PKA. Speculatively, TRPV1 multimerization might occur in lipid rafts in the plasma membrane due to the presence of to-date unidentified accessory proteins. Indeed, depletion of cholesterol can inhibit TRPV1 function and plasma membrane expression (54), supporting the notion that correct TRPV1 assembly to functional multimers occurs in discreet areas of the plasma membrane. Once the exact pathways involved are identified, these would present themselves as therapeutic targets to modulate TRPV1-mediated hyperalgesia.

In conclusion, our findings point toward a mechanism that allows for rapid and dynamic modulation of TRPV1 responses. Insertion of functional TRPV1 multimers into the plasma membrane from an intracellular store of inactive monomers as a consequence of activation of cAMP-dependent PKA allows for rapid potentiation and modulation of TRPV1 responses and conveys the additional advantage of minimizing disruption of intracellular calcium stores. This model further extends the complexity of cellular regulation of TRPV1 potentiation beyond the simple increase in trafficking that is suggested to mediate TRPV1 sensitization by protein kinase C (37–39). In addition, this system provides the capacity for rapid potentiation of TRPV1 responses without having to rely on transcriptional changes. Modification of the cellular mechanisms that lead to multimerization of TRPV1 channels and insertion of functional channels into the plasma membrane provides an endogenous pathway for adjusting hyperalgesia, without altering nociception itself. The propensity for dynamic regulation of potentiated TRPV1 responses is demonstrated by the ability of morphine to inhibit forskolin-mediated potentiation of TRPV1 responses by modulating TRPV1 multimerization and plasma membrane trafficking. This model may be of particular relevance to inflammation, where cellular cAMP levels are elevated, and the resultant increased activity of cAMP-dependent PKA contributes to the development of hyperalgesia (7, 27), but may also apply to other potentiation pathways.

Acknowledgments—We thank Dr. Alpha Yap (Institute for Molecular Biosciences, The University of Queensland, St Lucia, Australia) for the gift of the rabbit E-cadherin antibody. Part of the work was conducted in a UC Davis facility constructed with support from Research Facilities Improvement Program Grant C06-RR-12088-01 from the National Center for Research Resources.

REFERENCES

1. Taiwo, Y. O., Bjerknes, L. K., Goetzl, E. J., and Levine, J. D. (1989) *Neuroscience* **32,** 577–580
2. Rathee, P. K., Distler, C., Obreja, O., Neuhuber, W., Wang, G. K., Wang, S. Y., Nau, C., and Kress, M. (2002) *J. Neurosci.* **22,** 4740–4745
3. Caterina, M. J., Schumacher, M. A., Tominaga, M., Rosen, T. A., Levine, J. D., and Julius, D. (1997) *Nature* **389,** 816–824
4. Pomonis, J. D., Harrison, J. E., Mark, L., Bristol, D. R., Valenzano, K. J., and Walker, K. (2003) *J. Pharmacol. Exp. Ther.* **306,** 387–393
5. Walker, K. M., Urban, L., Medhurst, S. J., Patel, S., Panesar, M., Fox, A. J., and McIntyre, P. (2003) *J. Pharmacol. Exp. Ther.* **304,** 56–62
6. Caterina, M. J., Leffler, A., Malmberg, A. B., Martin, W. J., Trafton, J., Petersen-Zeitz, K. R., Koltzenburg, M., Basbaum, A. I., and Julius, D. (2000) *Science* **288,** 306–313
7. Hu, H. J., Bhave, G., and Gereau, R. T. (2002) *J. Neurosci.* **22,** 7444–7452
8. Bhave, G., Zhu, W., Wang, H., Brasier, D., Oxford, G., and Gereau, R. T. (2002) *Neuron* **35,** 721–731
9. Planells-Cases, R., Garcia-Sanz, N., Morenilla-Palao, C., and Ferrer-Montiel, A. (2005) *Pflugers Arch.* **451,** 151–159
10. Cabot, P. J., Carter, L., Gaiddon, C., Zhang, Q., Schäfer, M., Loeffler, J. P., and Stein, C. (1997) *J. Clin. Investig.* **100,** 142–148
11. Schafer, M., Imai, Y., Uhl, G. R., and Stein, C. (1995) *Eur. J. Pharmacol.* **279,** 165–169
12. Vetter, I., Wyse, B. D., Monteith, G. R., Roberts-Thomson, S. J., and Cabot, P. J. (2006) *Mol. Pain* **2,** 22
13. Kedei, N., Szabo, T., Lile, J. D., Treanor, J. J., Olah, Z., Iadarola, M. J., and Blumberg, P. M. (2001) *J. Biol. Chem.* **276,** 28613–28619
14. Morre, D. J., and Morre, D. M. (1989) *BioTechniques* **7,** 946–948, 950–954, 956–958
15. Hong, S., and Wiley, J. W. (2005) *J. Biol. Chem.* **280,** 618–627
16. Matsuura, B., Dong, M., Naik, S., Miller, L. J., and Onji, M. (2006) *J. Biol. Chem.* **281,** 12390–12396
17. von Wronski, M. A., Raju, N., Pillai, R., Bogdan, N. J., Marinelli, E. R., Nanjappan, P., Ramalingam, K., Arunachalam, T., Eaton, S., Linder, K. E., Yan, F., Pochon, S., Tweedle, M. F., and Nunn, A. D. (2006) *J. Biol. Chem.* **281,** 5702–5710
18. Ross, R. A., Gibson, T. M., Brockie, H. C., Leslie, M., Pashmi, G., Craib, S. J., Di Marzo, V., and Pertwee, R. G. (2001) *Br. J. Pharmacol.* **132,** 631–640
19. Dutertre, S., Croker, D., Daly, N. L., Andersson, A., Muttenthaler, M., Lumsden, N. G., Craik, D. J., Alewood, P. F., Guillon, G., and Lewis, R. J. (2008) *J. Biol. Chem.* **283,** 7100–7108
20. Cheng, W., Yang, F., Takanishi, C. L., and Zheng, J. (2007) *J. Gen. Physiol.* **129,** 191–207
21. Takanishi, C. L., Bykova, E. A., Cheng, W., and Zheng, J. (2006) *Brain Res.* **1091,** 132–139
22. Csordas, G., and Hajnoczky, G. (2001) *Cell Calcium* **29,** 249–262
23. Mohapatra, D. P., and Nau, C. (2003) *J. Biol. Chem.* **278,** 50080–50090
24. Wang, C., Hu, H. Z., Colton, C. K., Wood, J. D., and Zhu, M. X. (2004) *J. Biol. Chem.* **279,** 37423–37430
25. Rosenbaum, T., Awaya, M., and Gordon, S. E. (2002) *BMC Neurosci.* **3,** 4
26. Hebert, S. S., Daviau, A., Grondin, G., Latreille, M., Aubin, R. A., and Blouin, R. (2000) *J. Biol. Chem.* **275,** 32482–32490
27. Malmberg, A., Brandon, E., Idzerda, R., Liu, H., McKnight, G., and Basbaum, A. (1997) *J. Neurosci.* **17,** 7462–7470
28. Luo, H., Cheng, J., Han, J. S., and Wan, Y. (2004) *Neuroreport* **15,** 655–658
29. Tohda, C., Sasaki, M., Konemura, T., Sasamura, T., Itoh, M., and Kuraishi, Y. (2001) *J. Neurochem.* **76,** 1628–1635
30. Breese, N. M., George, A. C., Pauers, L. E., and Stucky, C. L. (2005) *Pain* **115,** 37–49
31. Amaya, F., Oh-hashi, K., Naruse, Y., Iijima, N., Ueda, M., Shimosato, G., Tominaga, M., Tanaka, Y., and Tanaka, M. (2003) *Brain Res.* **963,** 190–196
32. Mammone, T., Marenus, K., Maes, D., and Lockshin, R. A. (1998) *Skin Pharmacol. Appl. Skin Physiol.* **11,** 152–160
33. Murtaugh, M. P., Moore, W. T., Jr., and Davies, P. J. (1986) *J. Biol. Chem.* **261,** 614–621
34. Kuzhikandathil, E. V., Wang, H., Szabo, T., Morozova, N., Blumberg, P. M., and Oxford, G. S. (2001) *J. Neurosci.* **21,** 8697–8706
35. Jung, J., Hwang, S. W., Kwak, J., Lee, S. Y., Kang, C. J., Kim, W. B., and Kim, D. O. U. (1999) *J. Neurosci.* **19,** 529–538
36. Eun, S. Y., Jung, S. J., Park, Y. K., Kwak, J., Kim, S. J., and Kim, J. (2001) *Biochem. Biophys. Res. Commun.* **285,** 1114–1120
37. Huang, S. M., Bisogno, T., Trevisani, M., Al-Hayani, A., De Petrocellis, L., Fezza, F., Tognetto, M., Petros, T. J., Krey, J. F., Chu, C. J., Miller, J. D., Davies, S. N., Geppetti, P., Walker, J. M., and Di Marzo, V. (2002) *Proc. Natl. Acad. Sci. U. S. A.* **99,** 8400–8405
38. Kim, J. A., Kang, Y. S., and Lee, Y. S. (2005) *Arch. Pharm. Res.* **28,** 73–80
39. Mahieu, F., Owsianik, G., Verbert, L., Janssens, A., De Smedt, H., Nilius, B., and Voets, T. (2007) *J. Biol. Chem.* **282,** 3325–3336
40. Alebouyeh, M., Pourpak, Z., and Ahmadiani, A. (2002) *Cytokine* **19,** 102–105
41. Walker, J. S. (2003) *Adv. Exp. Med. Biol.* **521,** 148–160
42. Stein, A., Yassouridis, A., Szopko, C., Helmke, K., and Stein, C. (1999) *Pain* **83,** 525–532
43. Thomson, L. M., Terman, G. W., Zeng, J., Lowe, J., Chavkin, C., Hermes, S. M., Hegarty, D. M., and Aicher, S. A. (2008) *J. Pain* **9,** 11–19
44. Ballet, S., Mauborgne, A., Benoliel, J. J., Bourgoin, S., Hamon, M., Cesselin, F., and Collin, E. (1998) *Brain Res.* **796,** 198–208
45. Chao, C. C., Molitor, T. W., Close, K., Hu, S., and Peterson, P. K. (1993) *Int. J. Immunopharmacol.* **15,** 447–453
46. Clark, J. D., Shi, X., Li, X., Qiao, Y., Liang, D., Angst, M. S., and Yeomans, D. C. (2007) *Mol. Pain* **3,** 28
47. Mohapatra, D. P., and Nau, C. (2005) *J. Biol. Chem.* **280,** 13424–13432
48. Morenilla-Palao, C., Planells-Cases, R., Garcia-Sanz, N., and Ferrer-Montiel, A. (2004) *J. Biol. Chem.* **279,** 25665–25672
49. Esteban, J. A., Shi, S. H., Wilson, C., Nuriya, M., Huganir, R. L., and Malinow, R. (2003) *Nat. Neurosci.* **6,** 136–143
50. Chang, S. Y., Di, A., Naren, A. P., Palfrey, H. C., Kirk, K. L., and Nelson, D. J. (2002) *J. Cell Sci.* **115,** 783–791
51. Lee, S. Y. (2005) *Biochem. Biophys. Res. Commun.* **331,** 1445–1451
52. Chheda, M. G., Ashery, U., Thakur, P., Rettig, J., and Sheng, Z. H. (2001) *Nat. Cell Biol.* **3,** 331–338
53. Cayouette, S., and Boulay, G. (2007) *Cell Calcium* **42,** 225–232
54. Liu, M., Huang, W., Wu, D., and Priestley, J. V. (2006) *Eur. J. Neurosci.* **24,** 1–6